Rev. Adv. Mater. Technol., 2022, vol. 4, no. 4, pp. 1–16 DOI: 10.17586/2687-0568-2022-4-4-1-16

Review on Single-Mode Vertical-Cavity Surface-Emitting Lasers for High-Speed Data Transfer

S.S. Rochas*, Y.N. Kovach, P.E. Kopytov, A.V. Kremleva, A.Yu. Egorov

Institute of Advanced Data Transfer Systems, ITMO University, Kronverkskiy pr., 49, lit. A, St. Petersburg, 197101, Russia

Article history

Received December 13, 2022
Received in revised form December 20, 2022
Accepted December 22, 2022
Available online December 30, 2022

Abstract

Vertical-cavity surface-emitting lasers (VCSELs) are wide-spread laser sources for different applications in optical communication and sensing. The evolution of fabrication processes and new technological approaches allow to obtain high-Q single-mode VCSELs with data rates more than 100 Gbps. This review discusses basic designs and construction features of VCSELs that effect on their applications. The advances over the past 20 years for single-mode VCSELs of 850 nm, 1300 nm and 1550 nm wavelength ranges are presented.

Keywords: VCSEL; Fiber-optic communication lines; Telecommunications; Single-mode; Data rate

1. INTRODUCTION

The constant increase of the transmitted information volume leads to an increase in data processing and storage centers, as well as high-speed information and computing systems demand, which requires the generation of new light sources to increase the fiber-optic communication lines (FOCLs) bandwidth and reduce power consumption during data transmission, since data processing centers consumes about 1–3 % of global electricity capacity [1,2]. One of the rapidly growing directions of modern semiconductor optoelectronics research that solve this challenge is the development of vertical-cavity surface-emitting lasers (VCSELs).

VCSELs have significant advantages, in terms of comparison with edge-emitting lasers (EEL), such as small beam divergences [3] and small threshold currents [4,5], on the one hand, and relatively high temperature stability [6,7], on the other hand, which allow implementation of compact and energy-efficient laser radiation sources. Of great importance is the possibility to fabricate compact, single-mode (SM) generation over the entire current pumping range um-scale VCSELs crystals, which is due to the shorter length of the resonator [8]. Such devices do not suffer from light-current-voltage curve fractures as much as semiconductor lasers that switch to higher-order modes with a change in the pump current. The first commercial use of SM VCSELs was a computer mouse light source to increase tracking accuracy, due to the small beam divergence and symmetrical radiation pattern, and to reduce electricity consumption, compared to a LED based computer mouse [9]. Another application of SM VCSELs was atomic clocks for cesium and rubidium atoms [10].

Nowadays, VCSELs are firmly established as light sources in FOCLs [11]. The use of VCSELs operating at a wavelength of 850 nm for data transmission over distances of several hundred meters, i.e., for the first transparency window of quartz fiber, is widely spread [12]. This is due to high data transfer rates of devices and the relative simplicity of a monolithic laser heterostructures based on GaAs substrates [13]. SM operation long-wave (LW) VCSELs operating at a wavelength of 1300–1550 nm, which provide data transmission over distances of more than 1 kilometer through the second and third optical fiber transmission windows, are used in high-performance urban networks to reduce energy consumption and occupied space by electronic components [14,15]. Furthermore, SM LW VCSELs can be used for optical interconnections with a small radius of

* Corresponding author: S.S. Rochas, e-mail: stanislav_rochas@itmo.ru

© ITMO University, 2022

operation, for example, in transceivers or active optical cables [16], since the combination of SM and multimode fibers in data processing centers requires the use of wavelength-separated multiplexing devices to increase both the capacity and the accessibility of the data centers [17].

Lasing at the 1300–1550 nm range requires the use of an active region based on InP substrates [18]. In turn, the formation of monolithic VCSELs on InP substrates leads to a low contrast of refractive indices and poor thermal conductivity of distributed Bragg reflectors (DBR) layers and inefficient current and optical confinement [19], which leads to a decrease in the performance characteristics of the devices.

Other advantages of VCSELs are the prospect of silicon integration, which is of interest for silicon-based microwave photonics devices and their hybrid integration, and the possibility of a group manufacturing of devices on a wafer [20]. Thus, there is an opportunity to test VCSELs on the wafer, which reduces the cost of the devices, due to the crystals quantity per unit area, and allows to form two-dimensional matrices with many individual addressing emitters [21]. These matrices can be considered as sources for optical switching of electronic modules in high-performance computing systems [22]. For example, VCSELs are used in the Tsubame 3.0 supercomputer of the Tokyo Institute of Technology, and in cryogenic environments they reach bandwidth frequencies up to 40 and 50 GHz [23,24]. VCSELs matrices have found wide practical application in laser printers, where one laser has been replaced by a two-dimensional array of VCSELs, which has significantly increased the quality and speed of printing [25].

One of the VCSELs limiting factors is a relatively small output power (less than 10 mW), which is due to the small size of the devices and the small area of the active region (about 80 nm), taking part in the material gain [26]. However, in terms of telecommunication applications, VCSELs optical power values are high enough to meet the requirements for single-mode radiation sources.

Even though the data transmission markets grow steadily, VCSELs find new applications and occupying adjacent markets in such topical areas as infrared lighting [27], industrial heating, autonomous transport systems [28,29], various industrial, gas, biomedical sensors [30], and consumer products, such as smartphones with facial recognition systems, gestures and autofocus [31].

2. DISTRIBUTED BRAGG REFLECTORS

In VCSELs different construction of mirrors is used as in EELs, where light reflected from air-semiconductor interface creates positive feedback. To implement lasing in the vertical direction DBRs consisting of many pairs of semiconductor layers are used, so that a reflection coefficient of about 1 can be reached [32]. DBRs reflectivity depend on the number of paired layers and on the contrast of materials refractive indices [33]. There are several types of DBRs for VCSELs applications [34].

Monolithic semiconductor DBRs consist of arrayed AlGaAs layers with different content of Al. Such layers have a sufficiently high thermal conductivity [35], which makes it possible to dissipate heat from the VCSELs active region [36]. Such DBRs are the most common for telecommunication VCSELs due to their temperature characteristics and manufacturing processes which allow to grow thick AlGaAs lattice-matched layers without dislocation formation over the entire range of Al concentrations [37]. Nevertheless, monolithic semiconductor DBRs require lattice matching with VCSELs active regions and here they encounter some fundamental limitations for use in LW VCSELs [38]. The InP substrate, which is implemented in the epitaxial growth of LW VCSELs active regions, requires DBRs layers material system lattice-matched with InP, which is impractical due to the low contrast of refractive indices and poor thermal conductivity of these materials [39]. A practical solution may be the wafer fusion (WF) technique [40], which makes it possible to combine DBRs based on AlGaAs materials grown on a GaAs substrate and active region grown separately on an InP substrate [41,42]. However, it should be noted that WF requires additional high-tech equipment for defect-free fusion of active regions and semiconductor DBRs.

For the AlGaAs/GaAs material system it is also possible to form DBRs by lateral selective oxidation of AlGaAs layers with a high Al content [43]. Such $(AlGa)_xO_y$/GaAs DBRs are called oxidized DBRs. They provide a high level of reflection and a wide reflectance bandwidth while using fewer paired layers, compared to monolithic semiconductor DBRs, which is due to a significant difference in the refractive indices of the materials [44]. However, there is a problem of mechanical stability of such mirrors [45].

Another type of DBRs is dielectric DBRs, which are made of materials with higher refractive index than monolithic DBRs [44], so fewer paired layers are used to reach effective positive feedback. The most common paired layers are SiO_2/TiO_2 and SiO_2/Ta_2O_5. The main issue of such DBRs is a poor thermal conductivity, which makes it difficult to dissipate heat from the VCSEL active region [46]. It is also important that the use of dielectric DBRs requires implementation of intracavity (IC) contact layers, which complicates VCSELs fabrication processes [47]. Basic, hybrid structures with radiation output through the substrate are known. These structures combine different mirrors in one device to increase thermal conductivity, for example, the bottom transparent monolithic semiconductor DBR and the top dielectric DBR with a reflection coefficient close to 1 [48].

The peak reflectivity of the top (t) or bottom (b) mirror with number of layer pairs M_{Bt} or M_{Bb}, respectively, is written as [49]:

$$R_{t,b} = \left(\frac{1-b_{t,b}}{1+b_{t,b}}\right)^2, \quad (1)$$

with

$$b_t = \frac{n_s}{n_c}\left(\frac{n_1}{n_2}\right)^{2M_{Bt}}, \quad (2)$$

$$b_b = \frac{n_1^2}{n_c n_s}\left(\frac{n_1}{n_2}\right)^{2M_{Bb}}, \quad (3)$$

where n_c is refractive index of the cladding material, n_s is refractive index of the substrate (final layer), $n_{1,2}$ are refractive indices of DBR layers ($n_1 < n_2$).

The thickness of the DBR layers is determined by the expression:

$$d_{1,2} = \frac{\lambda_B}{4n_{1,2}}, \quad (4)$$

where λ_B is Bragg wavelength.

The DBRs reflectance bandwidth plateau of maximum reflectivity near the Bragg wavelength λ_B (stop zone/band) is defined as [50]:

$$\Delta\lambda_{stop} = \frac{2\lambda_B \Delta n_B}{\pi n_{gr}}, \quad (5)$$

where

$$\Delta n_B = |n_1 - n_2|, \quad (6)$$

and n_{gr} is group refractive index.

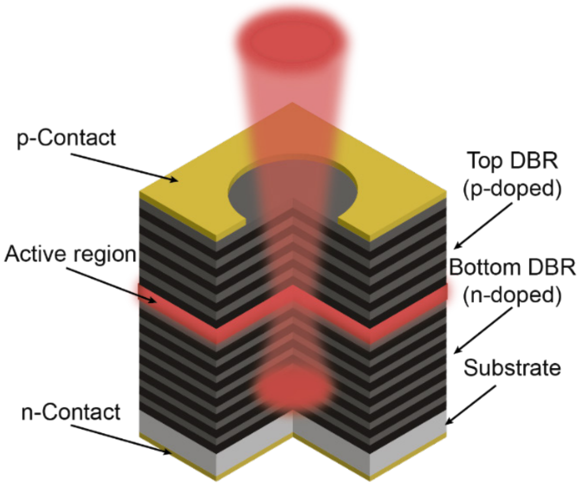

Fig. 1. VCSEL with electrically conductive DBRs.

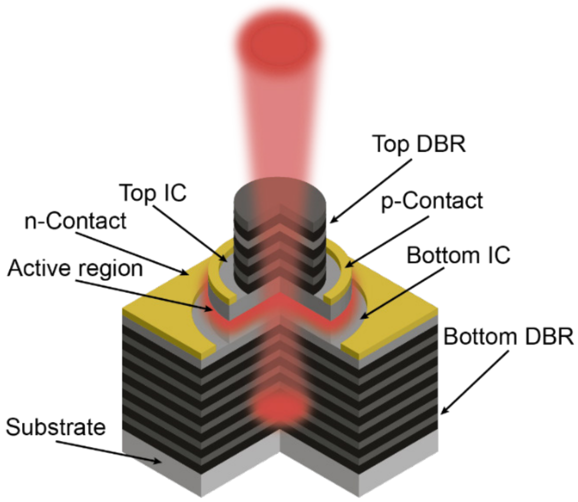

Fig. 2. VCSEL with IC contact layers.

3. CARRIERS INJECTION

One of the main differences in VCSELs designs is in the charge carrier injection into the active region [51]. It can be performed both through the DBRs [52] and the substrate or with the use of IC contact layers [53].

In the first case, metal contacts are applied to the top semiconductor mirror and to the bottom side of the substrate (Fig. 1). On the one hand, such design is easy to manufacture due to the planar technological process and it is actively used for 850 nm VCSELs [54]. On the other hand, the design requires high doping of the DBRs to reduce the ohmic resistance, which leads to the absorption of radiation in DBRs and to an increase in optical losses. This issue limits the use of this design for LW VCSELs [46] with a low optical gain. In addition, it is difficult to obtain small values of parasitic capacitance in doped DBRs, which limits the maximum frequency of devices [55].

The second case implies a design with a metallization deposition on the IC layers [56] sandwiching the active region (Fig. 2), which allows to use undoped DBRs. The use of IC layers significantly reduces optical losses on the mirrors, which is of interest for LW VCSELs [40]. However, this design complicates the manufacturing technology, since the creation of ohmic contacts on IC layers requires precision mesa etching due to small thickness of IC layers [57], as the use of thick layers leads to an increase in optical losses due to the free carrier absorption [58]. An important feature of this design is the possibility of flip-chip mounting, which is used in integrated matrices based on VCSELs [59] and silicon integrated circuits [60], since the contact pads are on the top side of the semiconductor heterostructure.

4. CURRENT CONFINEMENT

An increase in VCSELs quantum efficiencies and a decrease in their threshold and leakage currents are held by current confinement of the active region [61]. For energy-efficient and SM operation the current and the optical field must be confined in a way that the main optical mode excited by current with minimized optical losses [62]. The current aperture formation for a current confinement can be implemented by a selective oxidation of the active region (Fig. 3). The use of selective oxidation [63] solves the problem of current spreading between the *n*- and *p*-regions, eliminating non-radiative recombination and allows to form small dimension aperture [64]. Thus, the SM operation with large mesa etching sizes is possible. It should be noted that oxidation is not a precisely controlled process and causes mechanical instability within surrounding semiconductor layers [65].

Another way to form current aperture, which was mainly used at the early stages of VCSELs development, is a proton implantation [66]. The schematic view of the proton implanted VCSEL is shown in Fig. 4. The essence of the method is the implantation of protons through the upper DBR to form a waveguide and to accumulate charge carriers in the middle of the active region by reducing the lifetime of charge carriers in the implanted areas [67]. Such structures are relatively simple to manufacture but they have large threshold currents [68] and there is a risk of device degradation in case of accidental access of implants into the active region.

For a LW VCSELs it is possible to achieve current confinement with the use of a buried tunnel junction (BTJ) [69]. Tunnel junction (TJ) implies a *p-n* junction with a heavy doping ($>10^{19}$ cm^{-3}), where the charge carriers overcome the potential barrier while preserving their potential energy, and the concentrations of the dopant put the Fermi level much further into the conduction band of the n+ layer than the valence band of the p+ layer. When a non-zero voltage of any polarity is applied, a rapid increase in current between p and n layers of the tunnel junction follows. The BTJ concept (Fig. 5) for the LW VCSELs design is used to create a laterally structured TJ inside of a p-type section of the laser [70,71].

The BTJ diameter is limited by the diameter of the BTJ mesa and do not exceed the total diameter of the *p*-type section mesa. BTJ mesa is formed by selective etching of the upper n^+ layer to the p^+ layer [72]. The overgrowing (burying) of the TJ is carried out with a moderately doped *n*-type layer. Thus, within the p^+n^+ area of BTJ extremely low resistance is formed due to

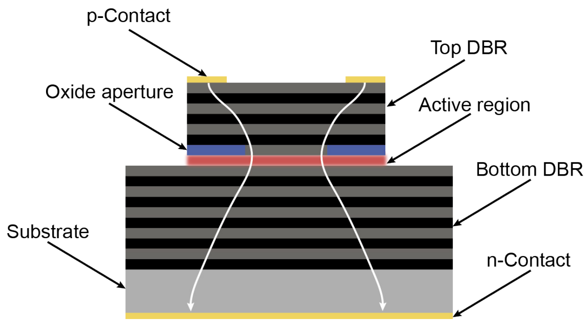

Fig. 3. Selectively-oxidized VCSEL.

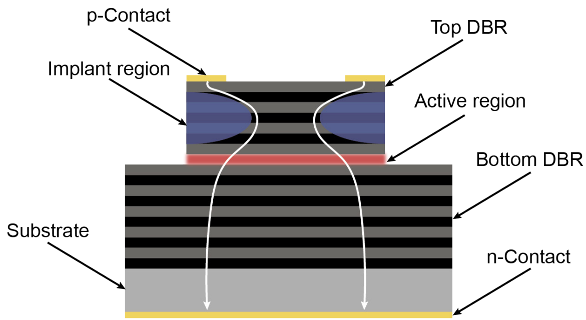

Fig. 4. Proton-implanted VCSEL.

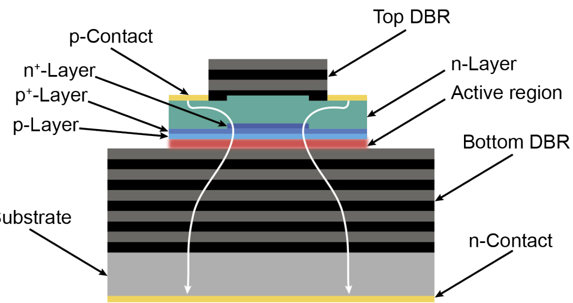

Fig. 5. VCSEL with a buried tunnel junction.

the tunnel effect and out of p^+n^+ area a reverse bias *p–n* junction is formed, which prevents the flow of current with the applied voltage.

The BTJ concept makes it possible to preserve the height difference between the BTJ region and periphery regions beyond it after burying when the depth of etching is $>\lambda/4n$, which provides a positive difference Δn_{eff} of the effective refractive index n_{eff} [73]

$$\frac{\Delta n_{eff}}{n_{eff}} = \frac{\Delta l_{opt}}{l_{opt}}, \qquad (7)$$

where l_{opt} and Δl_{opt} are the length of the optical resonator and the difference in the length of the optical resonator between the BTJ area and adjacent areas.

To bury the TJ it is possible to use not only the metalorganic vapour-phase epitaxy (MOCVD) method

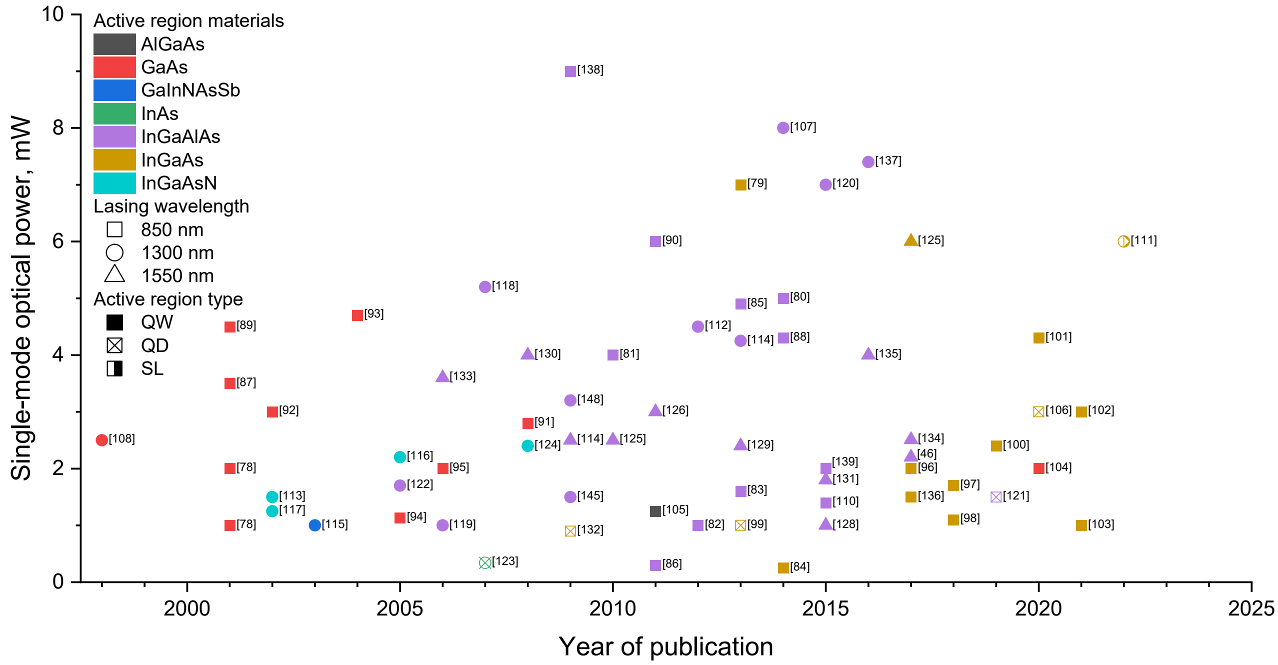

Fig. 6. Maximum output optical power achieved by VCSELs over the past 20 years.

but also molecular-beam epitaxy method, which eliminates the need of MOCVD setup [74]. However, the complete planarization of the overgrown surface does not occur, and a height difference corresponding to the TJ mesa depth on the overgrown surface is observed. This can lead to the «saturable absorber» effect, which is a significant increase in threshold current values and abrupt onsets of lasing (kink) [75].

5. ACTIVE REGION MATERIALS

Since the active regions of modern lasers are based on a heterojunction the choice of materials is limited due to the requirement of close materials' thermal expansion coefficients and crystal lattice constants to suppress the formation of defects at heterojunctions. For VCSELs fabrication A^3B^5 compounds are used, which are formed by a combination of aluminum, gallium, indium as group III elements on the one hand and phosphorus, arsenic, nitrogen and antimony as group V elements on the other hand. An important influence is exerted by the choice of dopants of II, VI, or IV groups of elements for additional charge carriers. As for the first practical implementation of VCSEL, the material of its active region was GaInAsP with charge carriers confinement realized by a double heterojunction [76]. Fig. 6 presents output optical power data for VCSEL three spectral bands reported over the past 20 years [46,55,78–140]. One of the most important features in the 850 nm VCSELs fabrication is a possibility of a single growth process of heterostructures containing both quantum wells (QWs) of the active region and high-Q upper and lower monolithic DBRs based on GaAs. In order to further increase the current density and to achieve a higher modal gain in lasing structures, it was proposed to use one or more QWs as an active region [77]. For example, in 2001 (Fig. 6) several 850 nm VCSELs with GaAs QW with output SM optical power of about 1 to 5 mW were demonstrated. Since 2010 a transition to another material of the active region — InGaAlAs —took place and since 2015 the most common material is the ternary solution of InGaAs, which is related to a non-radiative recombination decrease and development of technology to obtain strained QW with a significant lattice constant mismatch. The choice of active region materials for 850 nm telecommunication VCSELs do not significantly impact the SM output optical power value, which can be obtained from Fig. 6 , where the average value of studied devices is about 3–5 mW, since efficient operation in FOCLs can be carried out even at a power of 1 mW.

The use of ternary and quaternary solutions of A^3B^5 in QWs expands the spectral range of devices and makes it possible to achieve a higher optical gain at the same pumping due to a sharp change in the density of states near the edge of the quantum subband. Expanding the spectral range of VSCELs with GaAs-matched compounds such as InGaAsN(Sb) makes it possible to reach the LW range, but this does not lead to a high performance. Thus, in 2001, a 1300 nm VCSEL was demonstrated with a maximum output optical power of about 1 mW.

The most widely used LW VCSELs active regions are grown on InP substrates. The use of InGaAlAs QWs allowed to obtain SM output optical powers of 8, 7, 7.4 mW for 1300 nm VCSELs in 2014, 2015 and 2016, respectively [107,120,137]. For 1550 nm VCSELs the obtained SM output optical powers are significantly lower: 2.51 and 4 mW in 2017 [134] and 2016 [135], respectively. The use of InGaAs for 1550 nm VCSELs active regions allowed to obtain a SM output optical power of 6 mW in 2017 [125]. The main disadvantage of such active regions is the poor temperature stability, which, together with a lower reflectivity of DBRs based on InP, does not allow one to create monolithic devices such as 850 nm VCSELs based on GaAs. The practical solution of this issue is the use of dielectric mirrors or alternative approaches to create heterostructures, such as WF, which effectively combines the advantages of an active region based on InP and high-Q DBRs based on AlGaAs/GaAs materials.

SM operation at wavelengths of 1300 and 1550 nm requires the creation of an aperture with diameters ~ 4 and 6 μm for current and optical confinement, since the use of QWs leads to a charge carriers lateral diffusion in the active region, which increases the threshold current I_{th} . The use of quantum dots (QDs) solves the problem of charge carriers leakage and expands the VCSELs spectral range compared to QW-based VCSELs. However, due to the QDs array low surface density QD-based devices have a relatively low modal gain value. The studied QD-based VCSELs provided SM output optical powers less than 3 mW in 2020 [106]. Low values of SM output optical power are usually a consequence of additional QDs arrays to reach the modal gain, which leads to a large number of structural defects and requires complex methods to improve the quality of heterostructures.

As an alternative to active regions based on QWs and QDs active regions based on superlattices are known. In such structures minibands are formed [141], which are located both in the region of the QW and in the region of barrier layers. Thus, the width of the active region's effective part in such structures is greater than that of QW-based structures, which is due to an increase in standing light wave overlapping with the region that amplifying the light [142]. The demonstrated in 2022 [111] 1300 nm VCSEL with an InGaAs superlattice obtained by WF has an output optical power of 6 mW, which is superior to most of the LW QW-based VCSELs.

6. SMALL-SIGNAL MODULATION RESPONSE

Dynamics of VCSELs mode composition is described by a system of rate equations for the photon density of the mth mode N_m and the carrier density n as:

$$\frac{dn}{dt} = \frac{I}{qV} - \frac{n}{\tau_n} - \sum_m R_{st,m} N_m, \quad (8)$$

$$\frac{dN_m}{dt} = N_m \left(R_{st,m} - \tau_{ph,m}^{-1} \right) + R_{sp,m} K_{tot}, \quad (9)$$

where $R_{st,m}$ is stimulated recombination factor, $R_{sp,m}$ is spontaneous recombination factor, $\tau_{ph,m}$ is photon lifetime, K_{tot} is coefficient of total increase of spontaneous emission, I is injection current, q is elementary charge, V is VCSEL's active region volume, τ_n is carrier lifetime.

The contribution of spontaneous radiation can be neglected and as a result, the modulation transfer function linking the fluctuations of the photon density with the attenuation of the modeling current looks like this:

$$H(\nu) = \frac{\Delta \tilde{N}(\nu)}{\dfrac{\Delta \tilde{I}(\nu)}{q}} = \frac{A}{4\pi^2 \left(\nu_r^2 - \nu^2 \right) + i 2\pi\gamma\nu}, \quad (10)$$

with the amplitude factor

$$A = \frac{\eta_I v_{gr} \Gamma_r \bar{a} N_0}{V \left(1 + \varepsilon N_0 \right)}, \quad (11)$$

the damping coefficient

$$\gamma = \frac{1}{\tau_{sp}} + AV + \frac{\varepsilon N_0}{\tau_{ph} \left(1 + \varepsilon N_0 \right)}, \quad (12)$$

and the resonance frequency

$$\nu_r = \frac{1}{2\pi} \sqrt{A \frac{V}{\tau_{ph}} \left(1 + \frac{\varepsilon}{\tau_{sp} v_{gr} \Gamma_r \bar{a}} \right)}, \quad (13)$$

τ_{sp} is nonequilibrium carrier lifetime, ν is modulation frequency, v_{gr} is group velocity, Γ_r is relative confinement factor or gain enhancement factor, ε is gain compression factor, $\bar{a}$ is differential gain coefficient, η_I is current injection efficiency.

The damping coefficient can be rewritten as:

$$\gamma = K \nu_r^2 + \frac{1}{\tau_{sp}}, \quad (14)$$

where K is so-called K-factor

$$K = 4\pi^2 \left(\tau_{ph} + \frac{\varepsilon}{v_{gr} \Gamma_r \bar{a}} \right). \quad (15)$$

Its importance lies in the fact that the maximum –3dB modulation corner frequency $\left| H(\nu) \right|^2$ is related to the K-factor as:

$$\nu_{max} = \sqrt{2} \frac{2\pi}{K}. \quad (16)$$

This value characterizes the internal limit of laser modulation without any spurious effects. Main effects, acting as speed limits are self-heating and onset of multi-transverse-mode operation.

For applications in optical communication, it is of great interest to obtain a high modulation bandwidth at low operating currents. Taking an approximation for ν_r and neglecting the gain compression and relating the photon density N_0 to the output power P as $\hat{\eta}_d N_0 V_p \hbar\omega = \tau_{ph} P$ (with a photonic quantum efficiency for top and bottom emission $\hat{\eta}_d$, an effective volume occupied by the lasing mode V_p, a reduced Plank's constant $\hbar$ and an optical angular frequency ω) we get the expression:

$$\nu_r = D\sqrt{I - I_{th}}, \tag{17}$$

where the proportionality coefficient is often called the *D*-factor.

The modulation current efficiency factor (MCEF) determines the increase of –3dB corner frequency of $\left|H(\nu)\right|^2$ as:

$$MCEF = \frac{\nu_{-3dB}}{\sqrt{I - I_{th}}}. \tag{18}$$

Deviations from the ideal modulation mode occur due to parasitic elements found in the equivalent electrical circuit of the laser. They can be accounted for by a parasitic modulation transfer function $H_p(\nu)$, converting $H(\nu)$ into the total response:

$$H_t(\nu) = H(\nu) \cdot H_p(\nu). \tag{19}$$

The RC low-pass filter arising from the ohmic series resistance R and capacitance C can impose serious frequency restrictions. In this case, $H_p(\nu)$ is expressed as $1/\left(1 + i\nu/\nu_p\right)$, where $\nu_p = 1/(2\pi RC)$. Elements of an equivalent circuit can be derived from measurements of microwave impedance.

In general, the measured small-signal response of VCSEL is approximated by the function:

$$\left|H_t(\nu)\right|^2 = \frac{B\nu_r^4}{\left(\nu_r^2 - \nu^2\right)^2 + \left(\gamma\nu/(2\pi)\right)^2} \cdot \frac{1}{1 + \left(\nu/\nu_p\right)^2}, \tag{20}$$

with constant B.

The general behavior of $H_t(\nu)$ is shown in Fig. 7. As can be noted, it acts as a second-order low-pass filter. The modulation of VCSELs intensity follows current modulation up to ν_r, where the response is enhanced. However, when the resonance frequency is achieved the small-signal response drops off drastically. The frequency at which the electrical power response drops to half its DC value is ν_{3dB}, which for small current injection values is slightly greater than ν_r. And the actual peak position of $H_t(\nu)$, ν_p, becomes slightly smaller than ν_r with increasing current.

Long-lasted development of the 850 nm VCSEL growth technology already in the 2000s made it possible

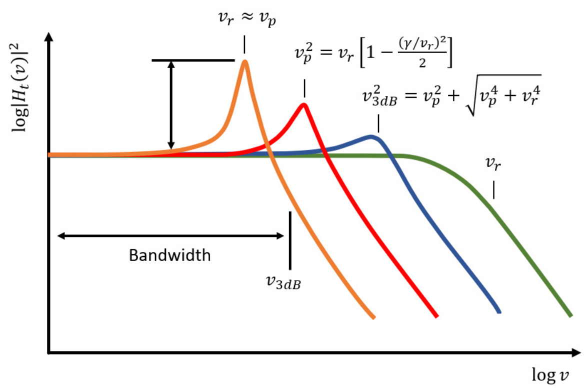

Fig. 7. Small-signal response for increasing values of resonance frequency with relationships between the peak, the resonance and the 3 dB-cutoff frequencies.

to introduce devices whose effective modulation frequency exceeds 15 GHz [63,78,95], and with the maximum achieved value is 21.5 GHz [78]. The following development of the production process of short-wavelength VCSELs made it possible to obtain a record value of 45 GHz in 2020, for which an electro-absorption modulator [104] was used.

For the next generation of VCSELs, where InGaAlAs was used as an active region, effective modulation frequencies at the level of 15–25 GHz [81,85–86,143–144] with a limiting value of 30 GHz [139] for 850 nm VCSELs became ordinary. As for LW VCSELs, maximum achieved values were 19 and 22 GHz, respectively [112]. Such an increase in frequency was realized using IC contacts, which made it possible to significantly reduce the capacitive component of the VCSEL, which was limiting the response time before.

Also, over the past five years, an improvement in the quality of heterostructures of devices based on quantum dots has been noted: their effective modulation frequency has almost doubled from 12–14 GHz [99,132] to 20–22 GHz [106,121].

As for the recent devices based on superlattices, they showed effective frequency modulation up to 8 GHz, however, such a low effective modulation frequency was associated not with the transition to a new design of the active region, but with a non-optimal doping level of the layers and with a large area of the reverse-biased *p*–*n* junction, which led to a significant increase in the capacity of the final VCSEL. In Fig. 8 the maximum effective frequency of VCSELs is noted for 850 nm, 1300 nm and 1550 nm [46, 55, 63, 78–82, 84–88, 90–102, 104–110, 112–125, 127–140, 143–154].

7. DATA RATES

In terms of digital modulation, time-dependent rate equations (8,9) must be solved including lateral variations of

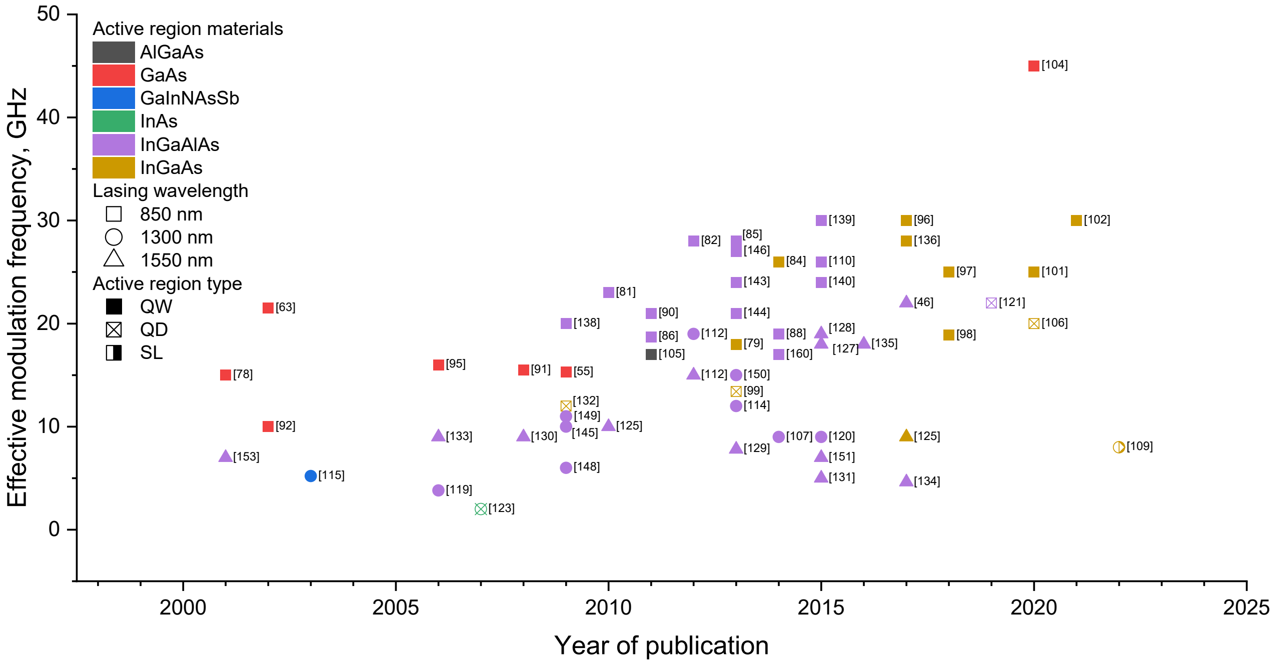

Fig. 8. Maximum effective modulation frequency of VCSELs over the past 20 years.

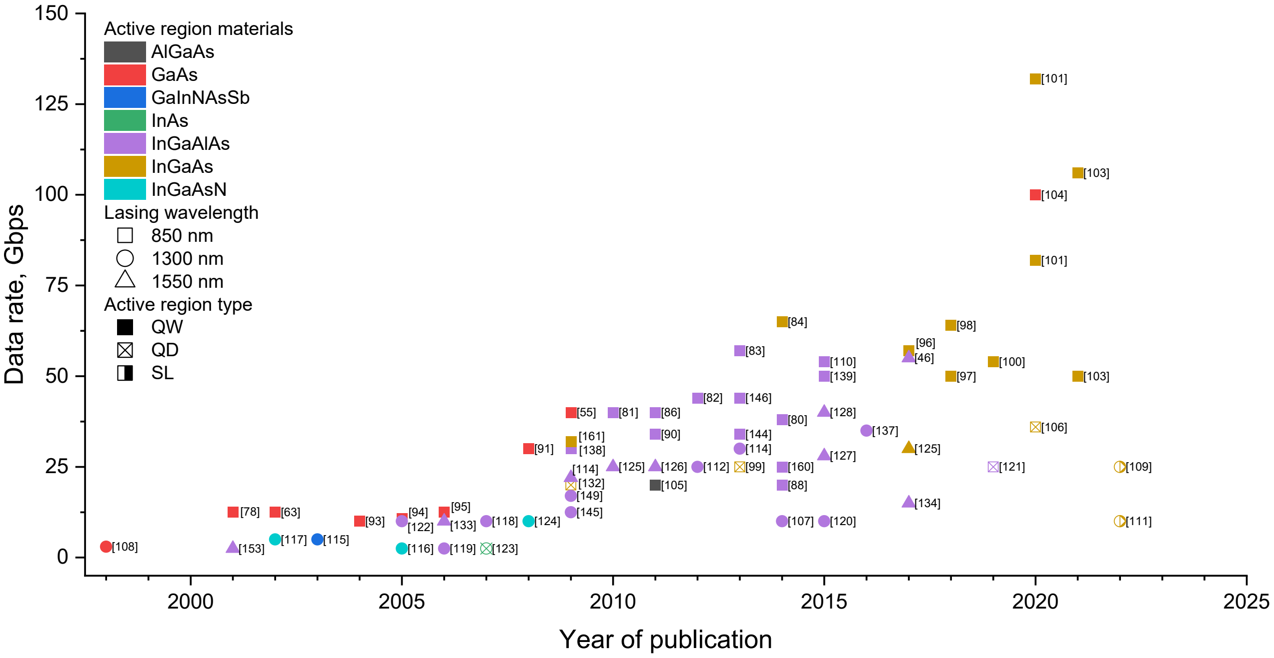

Fig. 9. Maximum data rate of VCSELs over the past 20 years.

particle densities and carrier diffusion, to consider numerical analysis of the large-signal modulation behavior [155]. There are several effects which impact on SM VCSELs modulation performance. One of them is turn-on delay, which is the time to build up carrier density in VCSEL active region to the threshold value [156]. The low VCSELs threshold allows to observe bias-free operation but the delay strongly depends on temperature, since a threshold current value rises [157]. This issue significantly limits bias-free uncooled VCSELs data rate. The spontaneous emission of active region causes fluctuations and deviation of turn-on delay called turn-on jitter, which is usually of about 10 ps [158]. Another issue is noises caused by a mode competition in case of a weak transverse mode or polarization suppression and electric parasitic [159]. The obtained VCSELs data rates are shown in Fig. 9 [55, 63, 80–84, 86, 88, 90, 91, 93–112, 114–123, 125–127, 132–134, 137–139, 144, 145, 149, 153, 160, 161].

For 850 nm VCSELs maximum data rate increased markedly over the past 20 years. The modernization of

GaAs QW-based SM VCSELs increased data rate from 10 Gbps in 2000 [78] up to 40 Gbps in 2010 [55] due to implementation of smaller aperture that provided higher resonance frequencies without significant increase in current density, which prevented overheating and increased lifetime of the devices, and technological fine-tunning of heterostructures to reduce parasitic resistance and capacitance. Further increase of data rate up to 60 Gbps in 2009–2015 is related to the use of strained InGaAlAs QWs [80–83,86,88,90,110,138–139,146], which reduced threshold currents and provided more efficient current and optical confinements. The use of QDs [99,106,132] as an active region was not justified, since constant cooling was required, and data rate was even less than in the case of QWs. The use of strained InGaAs QWs [96–98,100,103] without Al reduced non-radiative recombination, although it led to some issues with temperature characteristics, and has been most common for application since 2016, reaching data rates over 100 Gbps [101,103].

The development of LW VCSELs also affected data rate, which increased from 5 Gbps [115–117,119] up to 50 Gbps [46,128]. As with VCSELs for the first window of transparency the main progress in data rate is related to the use of strained InGa(Al)As QWs. Early works demonstrated VCSELs basically based on GaAs materials [108]. These devices did not exceed 15 Gbps and suffered from poor temperature stability and high threshold currents. The sufficient following progress is related with implementation of new approaches to fabricate high-Q VCSELs such as mesa etching of IC contact layers and heat-spreader, BTJ concept, flip-chip mounting, the use of hybrid metal-dielectric mirrors and WF with good thermal conductivity DBRs.

The use of superlattices as an active region for LW VCSELs seems to be perspective [109,111]. Even though the achievable speeds are not record-breaking, such devices demonstrate good temperature stability and are suitable for applications as uncooled laser radiation sources, but at the same time they require a set of complex high-tech processes to manufacture heterostructures.

8. CONCLUSIONS

In the present review we have summarizes types and features of mirrors and active regions designs, the ways of current confinement and carrier injection of VCSELs. We have also analyzed their characteristics for the past 20 years in terms of performance, such as single-mode optical power, modulation frequency and data rate for wavelength ranges of 850 nm, 1300 nm and 1550 nm. The most advanced and widespread is the combination of technologies such as WF with monolithic DBRs or dielectric DBRs in combination with IC contacts and the use of oxidation or BTJ to create an aperture for current and optical confinements.

The changes in active region material systems over the past 20 years allow to conclude that material systems have no significant impact in terms of SM optical power, which is due to a number of fundamental problems of VCSELs topology, such as charge leakage, issues with a temperature stability and limited sizes of aperture for a SM operation. In turn, with the use of the InGa(Al)As material system a significant progress was noted in maximum values of frequencies and data rates. Thus, to date, there has been an increase by about 2–3 times in the data rate for both 850 nm VCSELs and LW VCSELs.

The use of low-dimensional structures such as QDs does not find significant practical applications as strained QWs, despite an increase in frequencies values. However, new designs such as superlattice-based VCSELs are of interest, in particular, due to good temperature stability and record gain values.

ACKNOWLEDGMENTS

This study was done as a part of the research program of the scientific school "Theory and practice of advanced materials and devices of optoelectronics and electronics" (scientific school 5082.2022.4).

REFERENCES

[1] Y.M. Manaserh, M.I. Tradat, D. Bani-Hani, A. Alfallah, B.G. Sammakia, K. Nemati, M.J. Seymour, *Machine learning assisted development of IT equipment compact models for data centers energy planning*, Appl. Energy, 2022, vol. 305, art. no. 117846.

[2] H.B. Barua, K.C. Mondal, S. Khatua, *Green Computing for Big Data and Machine Learning*, in: Proc. CODS-COMAD 2022: 5th Joint International Conference on Data Science & Management of Data (9th ACM IKDD CODS and 27th COMAD), ed. by G. Dasgupta, Y. Simmhan, B.V. Srinivasan, S. Bhomwick, A. Singhee, M. Ramanath, N. Batra, Association for Computing Machinery, 2022, pp. 348–351.

[3] A.M. Hassan, X. Gu, M. Nakahama, S. Shinada, M. Ahmed, F. Koyama, *High power and high beam quality surface grating VCSEL*, in: Conference on Lasers and Electro-Optics, ed. by J. Kang, S. Tomasulo, I. Ilev, D. Müller, N. Litchinitser, S. Polyakov, V. Podolskiy, J. Nunn, C. Dorrer, T. Fortier, Q. Gan, C. Saraceno, OSA Technical Digest, 2021, art. no. STh1G.5.

[4] J.A. Lott, N.N. Ledentsov, V.M. Ustinov, N.A. Maleev, A.E. Zhukov, A.R. Kovsh, M.V. Maximov, B.V. Volovik, Z.I. Alferov, D. Bimberg, *InAs-InGaAs quantum dot VCSELs on GaAs substrates emitting at 1.3 µm*, Electron. Lett., 2000, vol. 36, no. 16, pp. 1384–1385.

[5] M.J. Miah, A. Al-Samaneh, A. Kern, D. Wahl, P. Debernardi, R. Michalzik, *Fabrication and characterization of low-threshold polarization-stable VCSELs for*

Cs-based miniaturized atomic clocks, IEEE J. Sel. Top. Quantum Electron., 2013, vol. 19, no. 4, art. no. 1701410.

[6] A. Mutig, J.A. Lott, S.A. Blokhin, P. Moser, P. Wolf, W. Hofmann, A.A. Nadtochiy, D. Bimberg, *Modulation characteristics of high-speed and high-temperature stable 980 nm range VCSELs operating error free at 25 Gbit/s up to 85 °C*, IEEE J. Sel. Top. Quantum Electron., 2011, vol. 17, no. 6, pp. 1568–1575.

[7] H. Li, P. Wolf, P. Moser, G. Larisch, J.A. Lott, D. Bimberg, *Temperature-stable, energy-efficient, and high-bit rate oxide-confined 980-nm VCSELs for optical interconnects*, IEEE J. Sel. Top. Quantum Electron., 2015, vol. 21, no. 6, art. no. 1700409.

[8] A. Larsson, *Advances in VCSELs for communication and sensing*, IEEE J. Sel. Top. Quantum Electron., 2011, vol. 17, no. 6, pp. 1552–1567.

[9] M. Grabherr, H. Moench, A. Pruijmboom, *VCSELs for Optical Mice and Sensing*, in: *VCSELs: Fundamentals, Technology and Applications of Vertical-Cavity Surface-Emitting Lasers*, ed. by R. Michalzik, Springer Series in Optical Sciences, vol. 166, Springer, Berlin, Heidelberg, 2013, pp. 521–538.

[10] D.K. Serkland, G.M. Peake, K.M. Geib, R. Lutwak, R.M. Garvey, M. Varghese, M. Mescher, *VCSELs for atomic clocks*, Proc. SPIE 6132, Vertical-Cavity Surface-Emitting Lasers X, 2006, art. no. 613208.

[11] S. Liverman, H. Bialek, A. Natarajan, A.X. Wang, *VCSEL array-based gigabit free-space optical femtocell communication*, J. Light. Technol., 2020, vol. 38, no. 7, pp. 1659–1667.

[12] H.Y. Kao, C.T. Tsai, Y.C. Chi, C.Y. Peng, S.F. Leong, H.Y. Wang, C.H. Cheng, W.L. Wu, H.C. Kuo, W.H. Cheng, C.H. Wu, G.R. Lin, *Long-term thermal stability of single-mode VCSEL under 96-Gbit/s OFDM transmission*, IEEE J. Sel. Top. Quantum Electron., 2019, vol. 25, no. 6, art. no. 1500609.

[13] A. Kern, A. Al-Samaneh, D. Wahl, R. Michalzik, *Monolithic VCSEL-PIN photodiode integration for bidirectional optical data transmission*, IEEE J. Sel. Top. Quantum Electron., 2013, vol. 19, no. 4, art. no. 6100313.

[14] J. Zou, S.A. Sasu, M. Lawin, A. Dochhan, J.P. Elbers, M. Eiselt, *Advanced optical access technologies for next-generation (5G) mobile networks*, J. Opt. Commun. Netw., 2020, vol. 12, no. 10, pp. D86–D98.

[15] S. Wassin, G.M. Isoe, R.R.G. Gamatham, A.W.R. Leitch, T.B. Gibbon, *Highly accurate pulse-per-second timing distribution over optical fibre network using VCSEL side-mode injection*, Proc. SPIE 10129, Optical Metro Networks and Short-Haul Systems IX, 2017, art. no. 101290G.

[16] N. Kohmu, M. Ishii, T. Ishigure, *High-density electrical and optical assembly for subminiature VCSEL-based optical engine*, IEEE Trans. Components Packag. Manuf. Technol., 2022, vol. 12, no. 1, pp. 27–36.

[17] G.M. Isoe, S. Wassin, A.W.R. Leitch, T.B. Gibbon, *60 Gbps 4-PAM VCSEL-based Raman assisted hyper-scale data centre: In context of spectral efficiency and reach extension*, Opt. Commun., 2018, vol. 428, pp. 164–168.

[18] B. Corbett, R. Loi, J. O'Callaghan, G. Roelkens, *Transfer printing for silicon photonics*, in: *Semiconductors and semimetals,* vol. 99, ed. by S. Lourdudoss, R.T. Chen, C. Jagadish, Elsevier, 2018, pp. 43–70.

[19] S. Spiga, M.C. Amann, *High-speed InP-based long-wavelength VCSELs*, in: *Green photonics and electronics. Nanoscience and technology*, ed. by G. Eisenstein, D. Bimberg, Springer, Cham, 2017, pp. 17–35.

[20] L. Carroll, J.-S. Lee, C. Scarcella, K. Gradkowski, M. Duperron, H. Lu, Y. Zhao, C. Eason, P. Morrissey, M. Rensing, S. Collins, H.Y. Hwang, P. O'Brien, *Photonic packaging: Transforming silicon photonic integrated circuits into photonic devices*, Appl. Sci, 2016, vol. 6, no. 12, art. no. 426.

[21] J. Bashir, E. Peter, S.R. Sarangi, *A survey of on-chip optical interconnects*, ACM Computing Surveys, 2019, vol. 51, no. 6, pp. 1–34.

[22] J.A. Tatum, G.D. Landry, D. Gazula, J.K. Wade, P. Westbergh, *VCSEL-based optical transceivers for future data center applications*, in: Optical Fiber Communications Conference, OSA Technical Digest (online), Optical Publishing Group, 2018, art. no. M3F.6.

[23] K. Iga, *VCSEL: born small and grown big*, Proc. SPIE 11263, Vertical External Cavity Surface Emitting Lasers (VECSELs) X, 2020, art. no. 1126302.

[24] W. Fu, H. Wu, D. Wu, M. Feng, D. Deppe, *Cryogenic oxide-VCSELs with bandwidth over 50 GHz at 82 K for next-gen high-speed computing*, in: Optical Fiber Communication Conference (OFC) 2021, ed. by P. Dong, J. Kani, C. Xie, R. Casellas, C. Cole, M. Li, OSA Technical Digest, Optica Publishing Group, 2021, art. no. Tu5C.4.

[25] N. Mukoyama, H. Otoma, J. Sakurai, N. Ueki, H. Nakayama, *VCSEL array-based light exposure system for laser printing*, Proc. SPIE 6908, Vertical-Cavity Surface-Emitting Lasers XII, 2008, art. no. 69080H.

[26] A.B. Ikyo, I.P. Marko, K. Hild, A.R. Adams, S. Arafin, M.C. Amann, S.J. Sweeney, *Temperature stable mid-infrared GaInAsSb/GaSb Vertical Cavity Surface Emitting Lasers (VCSELs)*, Sci. Rep., 2016, vol. 6, art. no. 19595.

[27] H. Moench, M. Frey, M. Grabherr, S. Gronenborn, R. Gudde, J. Kolb, M. Miller, A. Weigl, *VCSELs as light source for time-of-flight sensors*, Proc. SPIE 10122, Vertical-Cavity Surface-Emitting Lasers XXI, 2017, art. no. 1012204.

[28] Y. Li, J. Ibanez-Guzman, *Lidar for autonomous driving: The principles, challenges, and trends for automotive lidar and perception systems*, IEEE Signal Process. Mag., 2020, vol. 37, no. 4, pp. 50–61.

[29] Y. Kovach, A. Petrenko, S. Rochas, D. Shiryaev, A. Borodkin, E. Kolodeznyi, *Ring-shaped contamination detection system*, in: *International Youth Conference on Electronics, Telecommunications and Information Technologies*, Springer Proceedings in Physics, vol. 268, ed. by E. Velichko, V. Kapralova, P. Karaseov, S. Zavjalov, P. Angueira, S. Andreev, Springer, Cham, 2022, pp. 421–427.

[30] B.D. Padullaparthi, J.A. Tatum, K. Iga, *VCSEL Industry: Communication and Sensing*, Wiley, New York, 2021.

[31] S. Zhuo, Y. Wang, T. Xia, Y. Wu, W. Zheng, M. Sun, Z. Lin, P.Y. Chang, *A 200 MHz 14 W Pulsed Optical Illuminator with Laser Driver ASIC and On-chip DLL-Based Time Interpolator for Indirect Time-of-Flight Applications*, IEEE Trans. Circuits Syst. II Express Briefs, 2022, pp. 1.

[32] R. Michalzik, *VCSEL Fundamentals*, in: *VCSELs: Fundamentals, Technology and Applications of Vertical-Cavity Surface-Emitting Lasers,* ed. by R. Michalzik, Springer Series in Optical Sciences, vol 166, Springer, Berlin, Heidelber, 2013, pp. 19–75.

[33] R.M. France, J. Buencuerpo, M. Bradsby, J.F. Geisz, Y. Sun, P. Dhingra, M.L. Lee, M. A. Steiner, *Graded buffer Bragg reflectors with high reflectivity and transparency for metamorphic optoelectronics*, J. Appl. Phys., 2021, vol. 129, no. 17, art. no. 173102.

[34] M. Anaya, A. Rubino, M.E. Calvo, H. Míguez, *Solution processed high refractive index contrast distributed Bragg reflectors*, J. Mater. Chem. C, 2016, vol. 4, no. 20, pp. 4532–4537.

[35] I.O. Akhundov, D.M. Kazantsev, V.L. Alperovich, N.S. Rudaya, E.E. Rodyakina, A.V. Latyshev, *Formation and interaction of dislocation-induced and vicinal monatomic steps on a GaAs(001) surface under stress relaxation*, Scr. Mater., 2016, vol. 114, pp. 125–128.

[36] R.S. Adrain, J. Watson, *Laser microspectral analysis: A review of principles and applications*, J. Phys. D. Appl. Phys., 1984, vol. 17, no. 10, pp. 1915–1940.

[37] H. Gebretsadik, *Growth and characterization of defect-free GaAs/AlAs distributed Bragg reflector mirrors on patterned InP-based heterostructures*, J. Vac. Sci. Technol. B, 1998, vol. 16, no. 3, pp. 1417–1421.

[38] J. Boucart, C. Starck, F. Gaborit, A. Plais, N. Bouche, E. Derouin, J.C. Remy, J. Bonnet-Gamard, L. Goldstein, C. Fortin, D. Carpentier, P. Salet, F. Brillouet, J. Jacquet, *Metamorphic DBR and tunnel-junction injection. A CW RT monolithic long-wavelength VCSEL*, IEEE J. Sel. Top. Quantum Electron., 1999, vol. 5, no. 3, pp. 520–529.

[39] K.M. Gupta, N. Gupta, *Recent Advances in Semiconducting Materials and Devices*, in: *Advanced Semiconducting Materials and Devices. Engineering Materials*, ed. by K.M. Gupta, N. Gupta, Springer, Cham, 2016, pp. 531–562.

[40] M.E. Belkin, L. Belkin, A. Loparev, A.S. Sigov, V. Iakovlev, *Long Wavelength VCSELs and VCSEL-Based Processing of Microwave Signals*, in: *Optoelectronics - Materials and Devices*, ed. by S.L. Pyshkin, J. Ballato, InTechOpen, 2015.

[41] E. Kapon, A. Sirbu, *Power-efficient answer*, Nat. Photonics, 2009, vol. 3, no. 1, pp. 27–29.

[42] S.S. Rochas, I.I. Novikov, L.Y. Karachinsky, A.V. Babichev, S.A. Blokhin, V.N. Nevedomskii, K.O. Voropaev, A.Y. Egorov, *Wafer fusion technique features for near-IR laser sources*, J. Phys: Conf. Ser., 2021, vol. 2103, no. 1, art. no. 012107.

[43] G.D. Sulka, K. Hnida, *Distributed Bragg reflector based on porous anodic alumina fabricated by pulse anodization*, Nanotechnology, 2012, vol. 23, no. 7, art. no. 075303.

[44] T. Hamaguchi, H. Nakajima, N. Fuutagawa, *GaN-based vertical-cavity surface-emitting lasers incorporating dielectric distributed Bragg reflectors*, Appl. Sci, 2019, vol. 9, no. 4, art. no. 733.

[45] J.M. Dallesasse, D.G. Deppe, *III-V oxidation: Discoveries and applications in vertical-cavity surface-emitting lasers*, Proc. IEEE, 2013, vol. 101, no. 10, pp. 2234–2242.

[46] S. Spiga, W. Soenen, A. Andrejew, D.M. Schoke, X. Yin, J. Bauwelinck, G. Boehm, M.C. Amann, *Single-Mode High-Speed 1.5-µm VCSELs*, J. Light. Technol., 2017, vol. 35, no. 4, pp. 727–733.

[47] S.A. Blokhin, M.A. Bobrov, A.G. Kuzmenkov, A.A. Blokhin, A.P. Vasil'ev, Y.A. Guseva, M.M. Kulagina, I.O. Karpovsky, Y.M. Zadiranov, S.I. Troshkov, N.D. Prasolov, P.N. Brunkov, V.S. Levitsky, V. Lisak, N.A. Maleev, V.M. Ustinov, *A study of distributed dielectric bragg reflectors for vertically emitting lasers of the near-IR range*, Tech. Phys. Lett., 2016, vol. 42, no. 10, pp. 1049–1053.

[48] T. Gründl, P. Debernardi, M. Müller, C. Grasse, P. Ebert, K. Geiger, M. Ortsiefer, G. Böhm, R. Meyer, M.C. Amann, *Record single-mode, high-power VCSELs by inhibition of spatial hole burning*, IEEE J. Sel. Top. Quantum Electron., 2013, vol. 19, no. 4, art. no. 1700913.

[49] S.W. Corzine, R.H. Yan, L.A. Coldren, *A tanh substitution technique for the analysis of abrupt and graded interface multilayer dielectric stacks*, IEEE J. Quantum Electron., 1991, vol. 27, no. 9, pp. 2086–2090.

[50] K.J. Ebeling, *Integrated Optoelectronics*, Springer Berlin, Heidelberg, 1993.

[51] P. Maćkowiak, M. Wasiak, T. Czyszanowski, R.P. Sarzała, W. Nakwaski, *Designing guidelines for nitride VCSELs resonator*, Optica Applicata, 2002, vol. 32, no. 3. pp. 493–502.

[52] C. Wilsem, H. Temkin, L. Coldren, *Vertical-Cavity Surface-Emitting Lasers: Design, Fabrication, Characterization, and Applications*, Cambridge University Press, Cambridge, 2001.

[53] L. Mutter, V. Iakovlev, A. Caliman, A. Mereuta, A. Sirbu, E. Kapon, *1.3µm-wavelength phase-locked VCSEL arrays incorporating patterned tunnel junction*, Opt. Express, 2009, vol. 17, no. 10, pp. 8558–8566.

[54] C.C. Shen, T.C. Hsu, Y.W. Yeh, C.Y. Kang, Y.T. Lu, H.W. Lin, H.Y. Tseng, Y.T. Chen, C.Y. Chen, C.C. Lin, C.H. Wu, P.T. Lee, Y. Sheng, C.H. Chiu, H.C. Kuo, *Design, Modeling, and Fabrication of High-Speed VCSEL with Data Rate up to 50 Gb/s*, Nanoscale Res. Lett., 2019, vol. 14, no. 1, art. no. 276.

[55] A.N. AL-Omari, I.K. AL-Kofahi, K.L. Lear, *Fabrication, performance and parasitic parameter extraction of 850 nm high-speed vertical-cavity lasers*, Semicond. Sci. Technol., 2009, vol. 24, no. 9, art. no. 095024.

[56] A.C. Barone, *Short pulse generation from semiconductor lasers: characterization, modeling and applications*, Ingeniero en Electrónica, Madrid, 2011.

[57] R. Pu, E.M. Hayes, C.W. Wilmsen, K.D. Choquette, H.Q. Hou, K.M. Geib, *Comparison of techniques for bonding VCSELS directly to ICs*, J. Opt. A Pure Appl. Opt., 1999, vol. 1, no. 2, art. no. 324.

[58] A. Olsson, J. Tiira, M. Partanen, T. Hakkarainen, E. Koivusalo, A. Tukiainen, M. Guina, J. Oksanen, *Optical Energy Transfer and Loss Mechanisms in Coupled Intracavity Light Emitters*, IEEE Trans. Electron Devices, 2016, vol. 63, no. 9, pp. 3567–3573.

[59] R.F. Carson, M.E. Warren, P. Dacha, T. Wilcox, J.G. Maynard, D.J. Abell, K.J. Otis, J.A. Lott, *Progress in high-power high-speed VCSEL arrays*, Proc. SPIE 9766, Vertical-Cavity Surface-Emitting Lasers (VCSELs) XX, 2016, art. no. 97660B.

[60] J. Ferrara, W. Yang, L. Zhu, P. Qiao, C.J. Chang-Hasnain, *Heterogeneously integrated long-wavelength VCSEL using silicon high contrast grating on an SOI substrate*, Opt. Express, 2015, vol. 23, no. 3, pp. 2512–2523.

[61] W.J. Wang, C. Li, H.Y. Zhou, H. Wu, X.X. Luan, L. Shi, X. Guo, *Optimal oxide-aperture for improving the power conversion efficiency of VCSEL arrays*, Chinese Phys. B, 2015, vol. 24, no. 2, art. no. 024209.

[62] A. Larsson, E. Simpanen, J.S. Gustavsson, E. Haglund, E.P. Haglund, T. Lengyel, P.A. Andrekson, W.V. Sorin, S. Mathai, M. Tan, S.R. Bickham, *1060 nm VCSELs for*

long-reach optical interconnects, Opt. Fiber Technol., 2018, vol. 44, pp. 36–42.

[63] A. Haglund, C. Carlsson, J. Gustavsson, J. Halonen, A.G. Larsson, *Comparative study of the high-speed digital modulation performance of single- and multimode oxide confined VCSELs for free space optical interconnects*, Proc. SPIE 4649, Vertical-Cavity Surface-Emitting Lasers VI, 2002, pp. 272–280.

[64] D.G. Deppe, M. Li, X. Yang, M. Bayat, *Advanced VCSEL Technology: Self-Heating and Intrinsic Modulation Response*, IEEE J. Quantum Electron., 2018, vol. 54, no. 3, art. no. 2400209.

[65] Y. Zhang, J. Zhao, *Analysis of common failure causes in oxide VCSELs*, Proc. SPIE 12164, International Conference on Optoelectronic Materials and Devices (ICOMD 2021), 2022, art. no. 121641H.

[66] J.J. Pao, T.-C. Wu, W. Kyi, M. Riaziat, J.A. Lott, *Reliability and manufacturability of 25G VCSELs with oxide apertures formed by in-situ monitoring*, Proc. SPIE 10115, Advanced Fabrication Technologies for Micro/Nano Optics and Photonics X, 2017, art. no. 1011519.

[67] B. Kesler, T. O'Brien, J.M. Dallesasse, *Transverse mode control in proton-implanted and oxide-confined VCSELs via patterned dielectric anti-phase filters*, Proc. SPIE 10122, Vertical-Cavity Surface-Emitting Lasers XXI, 2017, art. no. 101220L.

[68] O. Ueda, S. Tomiya, *Grown-in defects and thermal instability affecting the reliability of lasers: III–Vs versus III-nitrides*, in: *Reliability of Semiconductor Lasers and Optoelectronic Devices*, ed. by R.W. Herrick, O. Ueda, Woodhead Publishing Series in Electronic and Optical Materials, Elsevier, 2021, pp. 177–238.

[69] J.A. Kearns, J. Back, N.C. Palmquist, D.A. Cohen, S.P. DenBaars, S. Nakamura, *Inhomogeneous Current Injection and Filamentary Lasing of Semipolar (2021) Blue GaN-Based Vertical-Cavity Surface-Emitting Lasers with Buried Tunnel Junctions*, Phys. Status Solidi A, 2020, vol. 217, no. 7, art. no. 1900718.

[70] J.S. Harris, H. Bae, T. Sarmiento, *GaInNAs(Sb) long-wavelength VCSELs*, in: *VCSELs: Fundamentals, Technology and Applications of Vertical-Cavity Surface-Emitting Lasers*, ed. by R. Michalzik, Springer Series in Optical Sciences, vol 166, Springer, Berlin, Heidelberg, 2013, pp. 353–377.

[71] A. Bachmann, K. Kashani-Shirazi, S. Arafin, M.C. Amann, *GaSb-based VCSEL with buried tunnel junction for emission around 2.3 μm*, IEEE J. Sel. Top. Quantum Electron., 2009, vol. 15, no. 3, pp. 933–940.

[72] S. Lee, C.A. Forman, J. Kearns, J.T. Leonard, D.A. Cohen, S. Nakamura, S.P. DenBaars, *Demonstration of GaN-based vertical-cavity surface-emitting lasers with buried tunnel junction contacts*, Opt. Express, 2019, vol. 27, no. 22, pp. 31621–31628.

[73] S. Arafin, A. Bachmann, M.C. Amann, *Transverse-mode characteristics of GaSb-based VCSELs with buried-tunnel junctions*, IEEE J. Sel. Top. Quantum Electron., 2011, vol. 17, no. 6, pp. 1576–1583.

[74] S. Blokhin, A. Babichev, A. Gladyshev, L. Karachinsky, I. Novikov, A. Blokhin, S. Rochas, D. Denisov, K. Voropaev, A. Ionov, N. Ledentsov, A. Egorov, *Wafer-fused 1300 nm VCSELs with an active region based on superlattice*, Electron. Lett., 2021, vol. 57, no. 18, pp. 697–698.

[75] S.A. Blokhin, M.A. Bobrov, A.A. Blokhin, A.P. Vasil'ev, A.G. Kuz'menkov, N.A. Maleev, S.S. Rochas, A.G. Gladyshev, A.V. Babichev, I.I. Novikov, L.Ya. Karachinsky, D.V. Denisov, K.O. Voropaev, A.S. Ionov, A.Yu. Egorov, V.M. Ustinov, *The Effect of a Saturable Absorber in Long-Wavelength Vertical-Cavity Surface-Emitting Lasers Fabricated by Wafer Fusion Technology*, Tech. Phys. Lett., 2020, vol. 46, no. 12, pp. 1257–1262.

[76] H. Soda, K.I. Iga, C. Kitahara, Y. Suematsu, *GaInAsP/InP surface emitting injection lasers*, Jpn. J. Appl. Phys., 1979, vol. 18, no. 12, art. no. 2329.

[77] Y. Arakawa, H. Sakaki, *Multidimensional quantum well laser and temperature dependence of its threshold current*, Appl. Phys. Lett., 1982, vol. 40, no. 11, pp. 939–941.

[78] F.H. Peters, M.H. MacDougal, *High-speed high-temperature operation of vertical-cavity surface-emitting lasers*, IEEE Photonics Technol. Lett., 2001, vol. 13, no. 7, pp. 645–647.

[79] J. Wang, M. Keever, Z.-W. Feng, T. Fanning, C. Chu, A. Sridhara, F. Hopfer, T. Sale, A.-N. Cheng, B. Shao, L. Ding, P. Wen, H.-H. Chang, C. Wang, D.C.W. Hui, L. Giovane, *28 Gb/s 850 nm oxide VCSEL development at Avago*, Proc. SPIE 8639, Vertical-Cavity Surface-Emitting Lasers XVII, 2013, art. no. 86390K.

[80] S.A. Blokhin, J.A. Lott, A. Mutig, G. Fiol, N.N. Ledentsov, M.V. Maximov, A.M. Nadtochiy, V.A. Shchukin, D. Bimberg, *Oxide-confined 850 nm VCSELs operating at bit rates up to 40 Gbit/s*, Electron. Lett., 2009, vol. 45, no. 10, pp. 501–503.

[81] P. Westbergh, J.S. Gustavsson, B. Kogel, A. Haglund, A. Larsson, A. Mutig, A. Nadtochiy, D. Bimberg, *850 nm VCSEL operating error-free at 40 Gbit/s*, in: 22nd IEEE International Semiconductor Laser Conference, ed. by Peter. M. Smowton, 2010, pp. 154–155.

[82] B. Kögel, J.S. Gustavsson, E. Haglund, R. Safaisini, A. Joel, P. Westbergh, M. Geen, R. Lawrence, A. Larsson, *High-speed 850 nm VCSELs with 28 GHz modulation bandwidth operating error-free up to 44 Gbit/s*, Electron. Lett., 2012, vol. 48, no. 18, pp. 1145–1147.

[83] P. Westbergh, E.P. Haglund, E. Haglund, R. Safaisini, J.S. Gustavsson, A. Larsson, *High-speed 850 nm VCSELs operating error free up to 57 Gbit/s*, Electron. Lett., 2013, vol. 49, no. 16, pp. 1021–1023.

[84] D.M. Kuchta, A.V. Rylyakov, C.L. Schow, J.E. Proesel, C. Baks, P. Westbergh, J. S. Gustavsson, A. Larsson, *64Gb/s Transmission over 57m MMF using an NRZ Modulated 850nm VCSEL*, in: Optical Fiber Communication Conference, OSA Technical Digest, Optica Publishing Group, 2014, art. no. Th3C.2.

[85] P. Westbergh, R. Safaisini, E. Haglund, J.S. Gustavsson, A. Larsson, A. Joel, *High-speed 850 nm VCSELs with 28 GHz modulation bandwidth for short reach communication*, Proc. SPIE 8639, Vertical-Cavity Surface-Emitting Lasers XVII, 2013, art. no. 86390X.

[86] F. Tan, C.H. Wu, M. Feng, N. Holonyak, *Energy efficient microcavity lasers with 20 and 40 Gb/s data transmission*, Appl. Phys. Lett., 2011, vol. 98, no. 19, art. no. 191107.

[87] S. Shinada, F. Koyama, N. Nishiyama, M. Arai, K. Iga, *Single high-order transverse mode 850 nm VCSEL with micromachined surface relief*, in: *Technical Digest. Summaries of papers presented at the Conference on Lasers and Electro-Optics*, Postconference Technical Digest (IEEE Cat. No. 01CH37170), 2001, pp. 106–107.

[88] R. Safaisini, E. Haglund, P. Westbergh, J.S. Gustavsson, A. Larsson, *20 Gbit/s data transmission over 2 km*

multimode fibre using 850 nm mode filter VCSEL, Electron. Lett., 2014, vol. 50, no. 1, pp. 40–42.

[89] F. Mederer, I. Ecker, J. Joos, M. Kicherer, H.J. Unold, K.J. Ebeling, M. Grabherr, R. Jager, R. King, D. Wiedenmann, *High performance selectively oxidized VCSELs and arrays for parallel high-speed optical interconnects*, IEEE Trans. Adv. Packag., 2001, vol. 24, no. 2, pp. 442–449.

[90] J.-W. Shi, W.-C. Weng, F.-M. Kuo, J.-I. Chyi, S. Pinches, M. Geen, A. Joel, *Oxide-relief vertical-cavity surface-emitting lasers with extremely high data-rate/power-dissipation ratios*, in: Optical Fiber Communication Conference/National Fiber Optic Engineers Conference 2011, OSA Technical Digest (CD), Optica Publishing Group, 2011, art. no. OThG2.

[91] R.H. Johnson, D.M. Kuchta, *30 Gb/s directly modulated 850 nm datacom VCSELs*, in: Conference on Lasers and Electro-Optics/Quantum Electronics and Laser Science Conference and Photonic Applications Systems Technologies, OSA Technical Digest (CD), Optica Publishing Group, 2008, art. no. CPDB2.

[92] R. Michalzik, F. Mederer, H. Roscher, M. Stach, H.J. Unold, D. Wiedenmann, R. King, M. Grabherr, E. Kube, *Design and communication applications of short-wavelength VCSELs*, Proc. SPIE 4905, Materials and Devices for Optical and Wireless Communications, 2002, pp. 310–321.

[93] F.-I. Lai, T.-H. Hsueh, Y.-H. Chang, H.-C. Kuo, S.C. Wang, L.-H. Laih, C.P. Song, H.P. Yang, *10 Gb/s single-mode vertical-cavity surface-emitting laser with large aperture and oxygen implantation*, Semicond. Sci. Technol., 2004, vol. 19, no. 8, pp. L86–L89.

[94] C.-L. Tsai, F.-M. Lee, F.-Y. Cheng, M.-C. Wu, S.-C. Ko, H.-L. Wang, W.-J. Ho, *Silicon oxide-planarized single-mode 850-nm VCSELs with TO package for 10 Gb/s data transmission*, IEEE Electron Device Lett., 2005, vol. 26, no. 5, pp. 304–307.

[95] T. Tanigawa, T. Onishi, S. Nagai, T. Ueda, *12.5-Gbps Operation of 850-nm Vertical-Cavity Surface-Emitting Lasers With Reduced Parasitic Capacitance by BCB Planarization Technique*, IEEE J. Quantum Electron., 2006, vol. 42, no. 8, pp. 785–790.

[96] A. Larsson, J.S. Gustavsson, P. Westbergh, E. Haglund, E.P. Haglund, E. Simpanen, T. Lengyel, K. Szczerba, M. Karlsson, *VCSEL design and integration for high-capacity optical interconnects*, Proc. SPIE 10109, Optical Interconnects XVII, 2017, art. no. 101090M.

[97] C.-H. Wu, W.-H. Cheng, M. Feng, C.-H. Wu, T.-Y. Huang, J. Qiu, W. Fu, C.-Y. Peng, T.-T. Shih, J.-J. Huang, H.-C. Kuo, G.-R. Lin, *50 Gb/s Error-Free Data Transmission Using a NRZ-OOK Modulated 850 nm VCSEL*, in: 2018 European Conference on Optical Communication (ECOC), 2018.

[98] H.-Y. Kao, C.-T. Tsai, S.-F. Leong, C.-Y. Peng, Y.-C. Chi, H.-Y. Wang, H.-C. Kuo, C.-H. Wu, W.-H. Cheng, G.-R. Lin, *Single-mode VCSEL for pre-emphasis PAM-4 transmission up to 64 Gbit/s over 100–300 m in OM4 MMF*, Photonics Res., 2018, vol. 6, no. 7, pp. 666–673.

[99] P. Moser, J.A. Lott, P. Wolf, G. Larisch, A. Payusov, N.N. Ledentsov, D. Bimberg, *Energy-Efficient Oxide-Confined 850-nm VCSELs for Long-Distance Multimode Fiber Optical Interconnects*, IEEE J. Sel. Top. Quantum Electron., 2013, vol. 19, no. 2, art. no. 7900406.

[100] T.-Y. Huang, J. Qiu, C.-H. Wu, H.-T. Cheng, M. Feng, H.-C. Kuo, C.-H. Wu, *A NRZ-OOK Modulated 850-nm VCSEL with 54 Gb/s Error-Free Data Transmission*, in: 2019 Conference on Lasers and Electro-Optics Europe & European Quantum Electronics Conference (CLEO/ Europe-EQEC), 2019.

[101] C.-Y. Huang, H.-Y. Wang, C.-Y. Peng, C.-T. Tsai, C.-H. Wu, G.-R. Lin, *Multimode VCSEL Enables 42-GBaud PAM-4 and 35-GBaud 16-QAM OFDM for 100-m OM5 MMF Data Link*, IEEE Access, 2020, vol. 8, pp. 36963–36973.

[102] N. Ledentsov Jr., Ł. Chorchos, O.Yu. Makarov, V.A. Shchukin, V.P. Kalosha, J.R. Kropp, J.P. Turkiewicz, C. Kottke, V. Jungnickel, R. Freund, N.N. Ledentsov, *Serial data transmission at 224 Gbit/s applying directly modulated 850 and 910 nm VCSELs*, Electron. Lett., 2021, vol. 57, no. 19, pp. 735–737.

[103] N. Ledentsov, L. Chorchos, O. Makarov, J.R. Kropp, V.A. Shchukin, V.P. Kalosha, J.P. Turkiewicz, N.N. Ledentsov, *Narrow spectrum VCSEL development for high performance 100G transceivers and increased transmission distance over multimode fiber*, Proc. SPIE 11704, Vertical-Cavity Surface-Emitting Lasers XXV, 2021, art. no. 117040P.

[104] K. Panajotov, R. Schatz, *Coupled-Cavity VCSEL with an Integrated Electro-Absorption Modulator: Small- and Large-Signal Modulation Analysis*, Appl. Sci., 2020, vol. 10, no. 17, art. no. 6128.

[105] N.N. Ledentsov, J.A. Lott, D. Bimberg, A. Mutig, G. Fiol, S.A. Blokhin, A.M. Nadtochiy, V.A. Shchukin, J. Kropp, I.I. Novikov, L.Ya. Karachinsky, M.V. Maximov, *High-speed single-mode quantum dot and quantum well VCSELs*, Proc. SPIE 7952, Vertical-Cavity Surface-Emitting Lasers XV, 2011, art. no. 79520J.

[106] H.R. Ibrahim, A.M.A. Hassan, M. Ahmed, F. Koyama, *Single-mode and High-speed Intracavity Metal Aperture VCSEL with Transverse Coupled Cavity Effect*, in: 2020 European Conference on Optical Communications (ECOC), 2020.

[107] D. Ellafi, V. Iakovlev, A. Sirbu, G. Suruceanu, Z. Mickovoc, A. Caliman, A. Mereuta, E. Kapon, *Impact of Selective DBR Surface Etching on the Performance of 1300 and 1500-nm Wafer-Fused VCSELs*, in: 2014 International Semiconductor Laser Conference, 2014, pp. 211–212.

[108] P. Schnitzer, R. Jäger, C. Jung, R. Michalzik, D. Wiedenmann, F. Mederer, K. J. Ebeling, *Biased and bias-free multi-Gb/s data links using GaAs VCSEL's and 1300-nm single-mode fiber*, IEEE Photonics Technol. Lett., 1998, vol. 10, no. 12, pp. 1781–1783.

[109] S.A. Blokhin, N. Ledentsov Jr., S.S. Rochas, A.V. Babichev, A.G. Gladyshev, L. Chorchos, O.Yu. Makarov, L.Ya. Karachinsky, I.I. Novikov, A.A. Blokhin, M.A. Bobrov, N.A. Maleev, V.V. Andryushkin, K.O. Voropaev, I.O. Zhumaeva, V.M. Ustinov, A.Yu. Egorov, N.N. Ledentsov, *1300-nm wafer-fused VCSELs with InGaAs/InAlGaAs superlattice-based active region*, Proc. SPIE 12020, Vertical-Cavity Surface-Emitting Lasers XXVI, 2022, art. no. 120200K.

[110] G. Stepniak, A. Lewandowski, J.R. Kropp, N.N. Ledentsov, V.A. Shchukin, N. Ledentsov Jr., G. Schaefer, M. Agustin, J.P. Turkiewicz, *54 Gbit/s OOK transmission using single-mode VCSEL up to 2.2 km MMF*, Electron. Lett., 2016, vol. 52, no. 8, pp. 633–635.

[111] S.A. Blokhin, A.V. Babichev, A.G. Gladyshev, L.Ya. Karachinsky, I.I. Novikov, A.A. Blokhin, M.A. Bobrov, N.A. Maleev, V.V. Andryushkin, D.V. Denisov, K.O. Voropaev, I.O. Zhumaeva, V.M. Ustinov, A.Yu. Egorov, N.N. Ledentsov, *High Power Single Mode 1300-nm Superlattice Based VCSEL: Impact of the Buried Tunnel Junction Diameter on Performance*, IEEE J. Quantum Electron., 2022, vol. 58, no. 2, art. no. 2400115.

[112] M. Müller, C. Grasse, M.C. Amann, *InP-based 1.3 μm and 1.55 μm short-cavity VCSELs suitable for telecom- and datacom-applications*, in: 2012 14th International Conference on Transparent Optical Networks (ICTON), 2012.

[113] A. Ramakrishnan, G. Steinle, D. Supper, C. Degen, G. Ebbinghaus, *Electrically pumped 10 Gbit/s MOVPE-grown monolithic 1.3 μm VCSEL with GaInNAs active region*, Electron. Lett., 2002, vol. 38, no. 7, pp. 322–324.

[114] W. Hofmann, M. Müller, A. Nadtochiy, C. Meltzer, A. Mutig, G. Böhm, J. Rosskopf, D. Bimberg, M.-C. Amann, C. Chang-Hasnain, *22-Gb/s Long Wavelength VCSELs*, Opt. Express, 2009, vol. 17, no. 20, pp. 17547–17554.

[115] H. Shimizu, C. Setiagung, M. Ariga, Y. Ikenaga, K. Kumada, T. Hama, N. Ueda, N. Iwai, A. Kasukawa, *1.3-μm-Range GaInNAsSb-GaAs VCSELs*, IEEE J. Sel. Top. Quantum Electron., 2003, vol. 9, no. 5, pp. 1214–1219.

[116] S. Bischoff, F. Romstad, M. Juhl, M. Madsen, J. Hanberg, D. Birkedal, *2.5 Gbit/s modulation of 1300 nm single-mode photonic crystal VCSELs*, in: 2006 Optical Fiber Communication Conference and the 2006 National Fiber Optic Engineers Conference, 2006.

[117] H. Riechert, A. Ramakrishnan, G. Steinle, *Development of InGaAsN based 1.3 μm VCSELs*, Semicond. Sci. Technol., 2002, vol. 17, no. 8, art. no. 892.

[118] A. Mircea, A. Caliman, V. Iakovlev, A. Mereuta, G. Suruceanu, C.A. Berseth, P. Royo, A. Syrbu, E. Kapon, *Cavity mode-gain peak tradeoff for 1320-nm wafer-fused VCSELs with 3-mW single-mode emission power and 10-Gb/s modulation speed up to 70 °C*, IEEE Photonics Technol. Lett., 2007, vol. 19, no. 2, pp. 121–123.

[119] M.R. Park, O.K. Kwon, W.S. Han, K.H. Lee, S.J. Park, B.S. Yoo, *All-epitaxial InAlGaAs-InP VCSELs in the 1.3-1.6-μm wavelength Range for CWDM band applications*, IEEE Photonics Technol. Lett., 2006, vol. 18, no. 16, pp. 1717–1719.

[120] D. Ellafi, V. Iakovlev, A. Sirbu, S. Grigore, Z. Mickovic, A. Caliman, A. Mereuta, E. Kapon, *Effect of Cavity Lifetime Variation on the Static and Dynamic Properties of 1.3-μm Wafer-Fused VCSELs*, IEEE J. Sel. Top. Quantum Electron., 2015, vol. 21, no. 6, art. no. 1700509.

[121] N. Ledentsov Jr., M. Agustin, V.A. Shchukin, J.-R. Kropp, N.N. Ledentsov, Ł. Chorchos, J.P. Turkiewicz, Z. Khan, C.-L. Cheng, J. W. Shi, N. Cherkashin, *Quantum dot 850 nm VCSELs with extreme high temperature stability operating at bit rates up to 25 Gbit/s at 150 °C*, Solid-State Electron., 2019, vol. 155, pp. 150–158.

[122] N. Nishiyama, C. Caneau, S. Tsuda, G. Guryanov, M. Hu, R. Bhat, and C.E. Zah, *10-Gb/s error-free transmission under optical reflection using isolator-free 1.3-μm InP-based vertical-cavity surface-emitting lasers*, IEEE Photonics Technol. Lett., 2005, vol. 17, no. 8, pp. 1605–1607.

[123] H.-C. Yu, J.-S. Wang, Y.-K. Su, S.-J. Chang, H.-C. Kuo, F.-I. Lai, Y.H. Chang, H.-P.D. Yang, *Low threshold current, low resistance 1.3 μm InAs-InGaAs quantum-dot VCSELs with fully doped DBRs grown by MBE*, Proc. SPIE 6484, Vertical-Cavity Surface-Emitting Lasers XI, 2007, art. no. 64840E.

[124] Y. Onishi, N. Saga, K. Koyama, H. Doi, T. Ishizuka, T. Yamada, K. Fujii, H. Mori, J. Hashimoto, M. Shimazu, T. Katsuyama, *100°C, 10 Gbps operation of buried tunnel junction GalnNAs VCSELs*, in: 2008 34th European Conference on Optical Communication, 2008, pp. 181–182.

[125] A.V. Babichev, L.Ya. Karachinsky, I.I. Novikov, A.G. Gladyshev, S.A. Blokhin, S. Mikhailov, V. Iakovlev, A. Sirbu, G. Stepniak, L. Chorchos, J.P. Turkiewicz, K.O. Voropaev, A.S. Ionov, M. Agustin, N.N. Ledentsov, A.Yu. Egorov, *6-mW Single-Mode High-Speed 1550-nm Wafer-Fused VCSELs for DWDM Application*, IEEE J. Quantum Electron., 2017, vol. 53, no. 6, art. no. 2400808.

[126] M. Muller, W. Hofmann, T. Grundl, M. Horn, P. Wolf, R.D. Nagel, E. Ronneberg, G. Bohm, D. Bimberg, M.C. Amann, *1550-nm High-Speed Short-Cavity VCSELs*, IEEE J. Sel. Top. Quantum Electron., 2011, vol. 17, no. 5, pp. 1158–1166.

[127] F. Karinou, N. Stojanovic, G. Goeger, C. Xie, M. Ortsiefer, A. Daly, R. Hohenleitner, B. Kögel, C. Neumeyr, *28 Gb/s NRZ-OOK using 1530-nm VCSEL, direct detection and MLSE receiver for optical interconnects*, in: 2015 IEEE Optical Interconnects Conference, 2015, pp. 20–21.

[128] W. Hofmann, M. Müller, P. Wolf, A. Mutig, T. Gründl, G. Böhm, D. Bimberg, M.-C. Amann, *40 Gbit/s modulation of 1550 nm VCSEL*, Electron. Lett., 2011, vol. 47, no. 4, pp. 270–271.

[129] Y. Rao, W. Yang, C. Chase, M.C.Y. Huang, D.P. Worland, S. Khaleghi, M.R. Chitgarha, M. Ziyadi, A.E. Willner, C.J. Chang-Hasnain, *Long-wavelength VCSEL using high-contrast grating*, IEEE J. Sel. Top. Quantum Electron., 2013, vol. 19, no. 4, art. no. 1701311.

[130] A. Syrbu, A. Mereuta, V. Iakovlev, A. Caliman, P. Royo, E. Kapon, *10 Gbps VCSELs with high single mode output in 1310nm and 1550 nm wavelength bands*, in: OFC/NFOEC 2008 - 2008 Conference on Optical Fiber Communication/National Fiber Optic Engineers Conference, 2008.

[131] K. Zogal, S. Paul, C. Gierl, P. Meissner, F. Kuppers, *Up to 12-Gbps transmission over 6.3-km SMF using a directly modulated bulk micromachined MEMS tunable VCSEL*, in: 2015 European Conference on Optical Communication (ECOC), 2015.

[132] J.A. Lott, V.A. Shchukin, N.N. Ledentsov, A. Stinz, F. Hopfer, A. Mutig, G. Fiol, D. Bimberg, S.A. Blokhin, L.Y. Karachinsky, I.I. Novikov, M.V. Maximov, N.D. Zakharov, P. Werner, *20 Gbit/s error free transmission with ~850 nm GaAs-based vertical cavity surface emitting lasers (VCSELs) containing InAs-GaAs submonolayer quantum dot insertions*, Proc. SPIE 7211, Physics and Simulation of Optoelectronic devices XVII, 2009, art. no. 721114.

[133] N. Nishiyama, C. Caneau, J.D. Downie, M. Sauer, C.E. Zah, *10-Gbps 1.3 and 1.55-μm InP-based VCSELs: 85°C 10-km error-free transmission and room temperature 40-km transmission at 1.55-μm with EDC*, in: 2006 Optical Fiber Communication Conference and the National Fiber Optic Engineers Conference, 2006.

[134] S. Paul, J. Cesar, M. Malekizandi, M.T. Haidar, N. Heermeier, M. Ortsiefer, C. Neumeyr, C. Gréus, M.H. Eiselt, I. Ibrahim, H. Schmidt, J. Schmidt, F. Küppers,

Towards a SFP+ module for WDM applications using an ultra-widely-tunable high-speed MEMS-VCSEL, Proc. SPIE 10122, Vertical-Cavity Surface-Emitting Lasers XXI, 2017, art. no. 1012209.

[135] A. Dochhan, N. Eiselt, R. Hohenleitner, H. Griesser, M. Eiselt, M. Ortsiefer, C. Neumeyr, J.J.V. Olmos, I.T. Monroy, J.P. Elbers, *56 Gb/s DMT transmission with VCSELs in 1.5 um wavelength range over up to 12 km for DWDM intra-data center connects*, in: ECOC 2016; 42nd European Conference on Optical Communication, 2016, pp. 391–393.

[136] J.-W. Shi, C.-C. Wei, J. Chen, N.N. Ledentsov, Y.-J. Yang, *Single-mode 850-nm vertical-cavity surface-emitting lasers with Zn-diffusion and oxide-relief apertures for > 50 Gbit/sec OOK and 4-PAM transmission*, Proc. SPIE 10122, Vertical-Cavity Surface-Emitting Lasers XXI, 2017, art. no. 101220F.

[137] A. Caliman, A. Sirbu, V. Iakovlev, A. Mereuta, P. Wolf, D. Bimberg, E. Kapon, *>25 Gbps direct modulation and data transmission with 1310 nm waveband wafer fused VCSELs*, in:Optical Fiber Communications Conference, OSA Technical Digest (online), Optica Publishing Group, 2016, art. no. Tu3D.1.

[138] P. Westbergh, J.S. Gustavsson, Å. Haglund, M. Skold, A. Joel, A. Larsson, *High-Speed, Low-Current-Density 850 nm VCSELs*, IEEE J. Sel. Top. Quantum Electron., 2009, vol. 15, no. 3, pp. 694–703.

[139] E. Haglund, P. Westbergh, J.S. Gustavsson, E.P. Haglund, A. Larsson, M. Geen, A. Joel, *30 GHz bandwidth 850 nm VCSEL with sub-100 fJ/bit energy dissipation at 25–50 Gbit/s*, Electron. Lett., 2015, vol. 51, no. 14, pp. 1096–1098.

[140] D.M. Kuchta, A.V. Rylyakov, C.L. Schow, J.E. Proesel, C.W. Baks, P. Westbergh, J.S. Gustavsson, A. Larsson, *A 50 Gb/s NRZ Modulated 850 nm VCSEL Transmitter Operating Error Free to 90 °C*, J. Light. Technol., 2015, vol. 33, no. 4, pp. 802–810.

[141] S.A. Nikishin, *III-nitride short period superlattices for deep UV light emitters*, Appl. Sci., 2018, vol. 8, no. 12, art. no. 2362.

[142] L.Ya. Karachinsky, I.I. Novikov, A.V. Babichev, A.G. Gladyshev, E.S. Kolodeznyi, S.S. Rochas, A.S. Kurochkin, Yu.K. Bobretsova, A.A. Klimov, D.V. Denisov, K.O. Voropaev, A.S. Ionov, V.E. Bougrov, A.Yu. Egorov, *Optical Gain in Laser Heterostructures with an Active Area Based on an InGaAs/InGaAlAs Superlattice*, Opt. Spectrosc., 2019, vol. 127, no. 6, pp. 1053–1056.

[143] D.M. Kuchta, C.L. Schow, A.V. Rylyakov, J.E. Proesel, F.E. Doany, C. Baks, B.H. Hamel-Bissell, C. Kocot, L. Graham, R. Johnson, G. Landry, E. Shaw, A. MacInnes, J. Tatum, *A 56.1Gb/s NRZ Modulated 850nm VCSEL-Based Optical Link*, in: Optical Fiber Communication Conference/National Fiber Optic Engineers Conference 2013, OSA Technical Digest (online), Optica Publishing Group, 2013, art. no. OW1B.5.

[144] J.-W. Shi, J.-C. Yan, J.-M. Wun, J. Chen, Y.-J. Yang, *Oxide-Relief and Zn-Diffusion 850-nm Vertical-Cavity Surface-Emitting Lasers With Extremely Low Energy-to-Data-Rate Ratios for 40 Gbit/s Operations*, IEEE J. Sel. Top. Quantum Electron., 2013, vol. 19, no. 2, art. no. 7900208.

[145] A. Gatto, A. Boletti, P. Boffi, C. Neumeyr, M. Ortsiefer, E. Ronneberg, and M. Martinelli, *1.3-µm VCSEL Transmission Performance up to 12.5 Gb/s for Metro Access Networks*, IEEE Photonics Technol. Lett., 2009, vol. 21, no. 12, pp. 778–780.

[146] P. Westbergh, R. Safaisini, E. Haglund, J.S. Gustavsson, A. Larsson, M. Geen, R. Lawrence, A. Joel, *High-Speed Oxide Confined 850-nm VCSELs Operating Error-Free at 40 Gb/s up to 85°C*, IEEE Photonics Technol. Lett., 2013, vol. 25, no. 8, pp. 768–771.

[147] R. Michalzik, K.J. Ebeling, M. Kicherer, F. Mederer, R. King, H. Unold, R. Jäger, *High-performance VCSELs for optical data links*, IEICE Trans. Commun., 2001, vol. E85-B, no. 5, pp. 1255–1264.

[148] A. Mereuta, G. Suruceanu, A. Caliman, V. Iacovlev, A. Sirbu, E. Kapon, *10-Gb/s and 10-km error-free transmission up to 100°C with 1.3-µm wavelength wafer-fused VCSELs*, Opt. Express, 2009, vol. 17, no. 15, pp. 12981–12986.

[149] M.C. Amann, W. Hofmann, *InP-based long-wavelength VCSELs and VCSEL arrays*, IEEE J. Sel. Top. Quantum Electron., 2009, vol. 15, no. 3, pp. 861–868.

[150] S. Spiga, M. Muller, M.C. Amann, *Energy-efficient high-speed InP-based 1.3 µm short-cavity VCSELs*, in: 2013 15th International Conference on Transparent Optical Networks (ICTON), 2013.

[151] S. Paul, C. Gierl, J. Cesar, Q.T. Le, M. Malekizandi, B. Kögel, C. Neumeyr, M. Ortsiefer, F. Küppers, *10-Gb/s direct modulation of widely tunable 1550-nm MEMS VCSEL*, IEEE J. Sel. Top. Quantum Electron., 2015, vol. 21, no. 6, art. no. 1700908.

[152] M. Ortsiefer, R. Shau, F. Mederer, R. Michalzik, J. Rosskopf, G. Böhm, F. Köhler, C. Lauer, M. Maute, M.-C. Amann, *High-speed modulation up to 10 Gbit/s with 1.55 µm wavelength InGaAlAs VCSELs*, Electron. Lett., 2002, vol. 38, no. 20, pp. 1180–1181.

[153] M. Ortsiefer, R. Shau, G. Böhm, F. Köhler, J. Roßkopf, G. Steinle, C. Degen, M. C. Amann, *High-temperature 2.5 Gb/s vertical-cavity surface-emitting lasers at 1.55 µm wavelength*, in: Proceedings 27th European Conference on Optical Communication (Cat. No.01TH8551), 2001, pp. 44–45.

[154] S. Paul, C. Gierl, J. Cesar, Q.T. Le, M. Malekizandi, F. Küppers, B. Kögel, J. Rosskopf, C. Gréus, M. Görblich, Y. Xu, C. Neumeyr, M. Ortsiefer, *High speed surface micromachined MEMS tunable VCSEL for telecom wavelengths*, in: 2015 Conference on Lasers and Electro-Optics (CLEO), OSA Technical Digest (online), Optica Publishing Group, 2015, art. no. AM3K.1.

[155] A. Ahmadian, *Laser diode modulation under large signal conditions*, in: 2013 21st Iranian Conference on Electrical Engineering (ICEE), 2013.

[156] A.Z. Goharrizi, G. Alahyarizadeh, *The study of temperature effect on the performance characteristics of the InGaN-based vertical cavity surface emitting laser (VCSEL) by solving the rate equations*, Int. J. Mod. Phys. B, 2016, vol. 30, no. 22, art. no. 1650150.

[157] J. Yan, J. Wang, C. Tang, X. Liu, M. Yang, W. Hao, Q. Zhuang, X. Cui, H. Zeng, *Performance Investigation of VCSEL-Based Voltage Probe and Its Applications to HPEM Effects Diagnosis of Embedded Systems*, IEEE Trans. Electromagn. Compat., 2018, vol. 60, no. 6, pp. 1923–1931.

[158] R. Shakhovoy, V. Sharoglazova, A. Udaltsov, A. Duplinskiy, V. Kurochkin, Y. Kurochkin, *Influence of Chirp, Jitter, and Relaxation Oscillations on Probabilistic*

Properties of Laser Pulse Interference, IEEE J. Quantum Electron., 2021, vol. 57, no. 2, art. no. 2000307.

[159] W.C. Lo, W.L. Wu, C.H. Cheng, H.Y. Wang, C.T. Tsai, C.H. Wu, G.R. Lin, *Effect of Chirped Dispersion and Modal Partition Noise on Multimode VCSEL Encoded with NRZ-OOK and PAM-4 Formats*, IEEE J. Sel. Top. Quantum Electron., 2022, vol. 28, no. 1, art. no. 1500409.

[160] S.A. Blokhin, L.Ya. Karachinsky, I.I. Novikov, A.S. Payusov, A.M. Nadtochiy, M.A. Bobrov, A.G. Kuzmenkov, N.A. Maleev, N.N. Ledentsov, V.M. Ustinov, D. Bimberg, *Degradation-robust 850-nm vertical-cavity surface-emitting lasers for 25Gb/s optical data transmission*, Semiconductors, 2014, vol. 48, no. 1, pp. 77–82.

[161] P. Westbergh, J.S. Gustavsson, A. Haglund, A. Larsson, F. Hopfer, G. Fiol, D. Bimberg, A. Joel, *32 Gbit/s multimode fibre transmission using high-speed, low current density 850 nm VCSEL*, Electron. Lett., 2009, vol. 45, no. 7, pp. 366–368.

УДК 621.373.826

Обзор на одномодовые вертикально-излучающие лазеры для высокоскоростной передачи данных

С.С. Рочас, Я.Н. Ковач, П.Е. Копытов, А.В. Кремлева, А.Ю. Егоров

Институт перспективных систем передачи данных, Университет ИТМО, Кронверкский пр., 49, лит. А, Санкт-Петербург 197101, Россия

Аннотация. Вертикально-излучающие лазеры (ВИЛ) являются широко распространенными источниками лазерного излучения для различных применений в волоконно-оптических линиях связи и в качестве сенсоров. Прогресс в технологиях изготовления и новые методы получения высококачественных ВИЛ позволили превысить скорости передачи данных более 100 Гбит/с. Данный обзор содержит описание основных конструктивных особенностей влияющих на характеристики ВИЛ. Представлены достижения за последние 20 лет в области одномодовых ВИЛ для передачи данных в диапазоне длин волн 850 нм, 1300 нм и 1550 нм.

Ключевые слова: вертикально-излучающий лазер; волоконно-оптические линии связи; телекоммуникации; одномодовый; скорость передачи данных